REGISTERED No. M. 3121

UNIVERSITY OF MICHIGAN
JAN 11 1955
PHYSICS LIBRARY

PROCEEDINGS

OF THE

INDIAN ACADEMY OF SCIENCES

VOL. XL] *SECTION A* [NO. 4

OCTOBER 1954

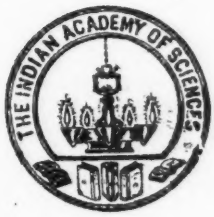

Price Rs. 2 or 3 Sh. ***Annual Subscription Rs. 18***

PRINTED AT THE BANGALORE PRESS, BANGALORE CITY, BY C. VASUDEVA RAO,
SUPERINTENDENT AND PUBLISHED BY THE INDIAN ACADEMY OF
SCIENCES, BANGALORE.

ON THE CONSTRUCTION OF LARGE NUCLEAR EMULSION BLOCK DETECTORS

By R. R. Daniel, G. Friedmann, D. Lal, Yash Pal and B. Peters, F.A.Sc.
(Tata Institute of Fundamental Research, Bombay 1, India)

Received September 24, 1954

CONTENTS

		Page
I.	Introduction	151
II.	Technical Problems Connected with the Construction of Large Emulsion Block Detectors ..	153
III.	A New Reference System for Plate Alignment ..	154
IV.	Acknowledgements	157

I. Introduction

All emulsion block detectors whose construction has been reported so far have the shape of flat slabs whose thickness is by a factor of about six, smaller than one or both lateral dimensions. Such a shape is usually advantageous in the study of artificially produced nuclear phenomena where the radiation incident on the detector has a strongly preferred spatial direction. On the other hand, when exposed to cosmic radiation at high altitudes, which usually shows little directional preference, the "best" shape depends strongly on the type of phenomena to be investigated. In general a flat detector is suitable for studying the incident radiation, but the spherical or cubical detector is much more advantageous when studying secondary particles, irrespective of whether the latter are stable or unstable, neutral or charged. Roughly:—

The number of incident particles recorded is larger in a flat detector than a cubical one of equal volume.

The number of nuclear interactions per unit volume produced by the incident radiation is nearly independent of the detector shape as long as the detector is not large compared to a nuclear mean free path.

It follows that in a cubical detector the average potential path length of primaries is larger, often appreciably larger, than in flat detectors. This will also be true for low energy secondaries ejected isotropically from stars and for tertiary particles emitted from unstable particles

which have been brought to rest. If the incident radiation is isotropically distributed over the upper hemisphere it will also apply to fast secondaries which preserve more or less the direction of the primaries.

Thus, for a given primary star population the cubical detector will in general contain a larger fraction of secondary and tertiary particles which come to rest, a larger fraction of decays in flight and also a larger fraction of nuclear interactions produced by secondary particles. This last feature may be of great importance in the study of *K*-mesons and Hyperons if, as some experimental data now suggest, π-meson produced stars are richer in *K*-mesons and Hyperons than nucleon produced stars.*

For this reason we decided last Fall to begin the construction of an emulsion block detector whose thickness is comparable with its other dimensions.

In deciding the over-all dimension of the detector one has to make a compromise between what is desirable and what is practical. Since part of our objective was to get precise information on the mass and decay schemes of various *K*-mesons and Hyperons it would have been best to have a detector with a stopping power of at least 100 grams/cm.^{2}, *i.e.*, linear dimension of 25 cms. This is needed because at present exact information on the energy and the nature of charged decay products from unstable particles is only obtainable if their range can be measured.

* It can easily be shown that for an isotropic flux, the average potential track length of primaries in a rectangular block is independent of its orientation and equals $\frac{4V}{S}$, where V and S are its volume and surface area respectively. For secondaries, if they also have angular isotropy, the mean potential length, is half as large: $\langle L \rangle = \frac{2V}{S}$.

In the table below we have given the mean length $\langle L \rangle$ of the trajectories of secondary and tertiary particles as well as the approximate ratio (R) of stars produced by primary and by secondary particles in our Blocks, and in those of various European Laboratories (Sardinia flights, 1953). In order to calculate R we have assumed an average of 3 fast secondaries, with interaction length of 27 cms. per primary star.

Block	No. of Emulsion Sheets	Lateral Dimensions cm.	$\langle L \rangle$ cm.	R
Bombay No. 1 ..	24	10×15	1·15	7·75
Bombay No. 2 ..	125	15×15	3·75	2·4
Bombay No. 3 ..	200	15×15	4·60	1·95
Sardinia ..	40	15×15	1·80	5·0

An elementary calculation, however, reveals that cubical shapes and linear dimensions of the order of 25 cms. when combined will give an emulsion block which will not only present a very heavy load compared to customary balloon borne equipment, but will also be so expensive that the risk seems justified only after one can be confident that all technical problems involved in the construction of such emulsion block detectors have been successfully solved. We have, therefore, decided to reduce the lateral dimensions rather than compromise too much on the shape, and have exposed two stacks of square emulsion sheets 15×15 cm., $600\,\mu$ thick. One stack consisted of 200 emulsion sheets and had, therefore, a thickness of 12 cms., the other one contained 125 emulsion sheets corresponding to 7·5 cms. thickness.

II. Technical Problems Connected with the Construction of Large Emulsion Block Detectors

In an earlier paper[1] a description was given of the technique used in constructing and aligning our first emulsion block detector consisting of 24 sheets of emulsion. We now consider only those technical problems which were not satisfactorily solved previously and those which arise because of the increased size of the detector. These are of two types.

One set of difficulties, by no means negligible, is connected simply with the larger number of plates to be handled. Apart from the more than normal precaution to be taken in order to recover such valuable equipment after the balloon flight, it is necessary to organize the processing, cutting and aligning in such a way that it can be done in a reasonable number of man-hours. Furthermore, since for many problems the usefulness of the emulsion block detector is greatly reduced if a single emulsion sheet is spoiled, destroyed or lost, it becomes necessary to instal automatic safety devices for the processing operation.

The second set of difficulties is connected with the fact that a large stack is only fully useful if the tracing of particles is possible even when their tracks have minimum ionisation and, therefore, no longer stand out against the unavoidable background of electron tracks. This implies that the mounted sheets must be so well aligned that when successive slides are placed into the microscope stage holder, one looks at corresponding points of the adjacent emulsion surfaces with an error which should not exceed about $20\,\mu$. It is of course true that minimum tracks can be traced even though the alignment error is of the order of 100–$200\,\mu$, but in that case elaborate

[1] D. Lal, Yash Pal and B. Peters, *Proc. Ind. Acad. Sci.*, 1953, **38**, 277.

plots of other tracks in the region are necessary, and the time required to trace a minimum ionisation track through 50 or 100 plates becomes prohibitive.

Reference (1) describes an aligning procedure in which the microscope slides were placed on plastic frames and adjusted under the microscope into their proper relative positions; the tracks of heavy primaries were used for establishing corresponding points on adjacent surfaces. The accuracy achieved was limited by:

(*a*) Emulsion distortion. The two adjacent plates may have been brought back exactly to the relative position they occupied before exposure. Nevertheless, subsequent distortion could move a point on the air surface away from its proper position, and thus when exchanging plates in the slide holder, the continuation of a given track may not be found where it was expected.

(*b*) In our first block detector there were gaps between adjacent emulsion sheets during exposure which varied between 100–150 μ. These were due to the tissue papers which were placed between emulsions in order to prevent sticking, and also to the lack of compression between the sheets in the block. Compression was then intentionally kept small so as to avoid damaging or blackening the emulsion surfaces.

(*c*) The alignment of each microscope slide required about 20 minutes. Any five minutes saved by improving the procedure would constitute a saving of nearly 200 man-hours on large detectors.

III. A New Reference System for Plate Alignment

In order to overcome the difficulties listed above we placed between the emulsions a network of nylon threads of 18 μ diameter, which were made α-particle active. These threads produced lines on the emulsion surface along which α-particles were emitted and the line's center could be easily determined with an accuracy of 5 μ. α-particles penetrate deep enough under the surface to prevent their being rubbed off, and yet not so deep as to interfere with scanning and measurements. Since the markings are identical on contiguous surfaces of adjacent emulsions, the exact mis-alignment in any region of the plate due to distortion or other causes can be measured quickly and accurately.

The nylon fibres themselves proved adequate for keeping the emulsion sheets separated and preventing their sticking together. Thus, paper sheets between emulsions could be eliminated. It was possible to exert strong

pressure by means of screws on the assembled emulsion sheets before exposure. The gaps between emulsion sheets were now small and found to vary only between 25 and 35 μ.

Finally instead of heavy primary tracks the grid lines imprinted on adjacent emulsion surfaces were used for the purpose of plate alignment and with the help of the double microscope set up, described below, the time necessary for alignment could be reduced by a factor of four. The details of the procedure were as follows:

(*a*) *Preparation of the Polonium Solution*

It is essential to prepare a sample of Polonium free from β-activity since otherwise the emulsions will be fogged.* Polonium was extracted chemically from 10 old radon needles and the extract was found to contain about 30 microcuries. The purity was tested by counters as well as nuclear emulsions. The Polonium was then brought into solution of 15 litres by adding water.

(*b*) *Preparation of the Nylon Grids*

The nylon fibres used were so fine that they can only be seen with good illumination, against a dark background. In order to place them between emulsion sheets in a darkroom it is necessary to mount them in such a way that they can be handled without difficulty. For this reason we constructed grids.

The nylon fibres were obtained from strands of nylon rope and were found to have a uniform diameter of 18 μ. They were stuck with fast drying glue, on thick cardboard window frames, the inside dimensions of which were $9'' \times 9''$. The grid spacing was 1 cm. throughout. The cardboard edges were then immersed in liquid hot paraffin wax, taking care that the wax did not touch the inside 6" square of the grid. 600 such grids were produced.

The frames were now soaked in the Polonium solution for a period of six hours and dried in air. They were then transferred to smaller cardboard frames with inside dimensions of $6\frac{1}{4}'' \times 6\frac{1}{4}''$. The cardboard had a thickness of only 500 μ. After transferring the grid to the new frame, using again fast drying cement, the contaminated outer frame was cut off with a sharp blade. The grids were then ready for use.

(*c*) *Assembly of the Emulsion Block*

To keep the emulsions of the stack in position and to have them roughly aligned during the entire exposure, we built a special frame consisting of a

* We are indebted to Dr. H. D. Sharma for preparing the solution.

wooden base plate into which five brass rods were fixed. Two of the rods were made eccentric and permitted the emulsions to be brought in flush with the two edges defined by the remaining rods. The frames covering the grids were punched at appropriate places on their inner edges to fit snugly outside the rods. Each emulsion was alternated with a grid and the entire assembly was pressed down firmly with a second wooden board passing through the five rods. The stacks were flown with the sheets in a vertical position.

(*d*) *Processing*

Mounting and processing procedures did not differ from those previously described. One observation may, however, be of some interest to other laboratories. We found that the probability of getting bubbles during development depends to a large extent on the quality of the treated glass plates used for mounting. A sheet of emulsion cut in two, and mounted with identical procedures, one on a freshly prepared glass sheet and one on a glass sheet which had been exposed to the atmosphere for some time, yielded two plates of which one was free from bubbles and the other very heavily effected. Thus, by using fairly fresh glass plates and storing them in a refrigerator we reduced in our large blocks, the number of bubbles to the tolerable value of about one per 75 sq. cm.

It may also be worth mentioning that in an attempt to reduce distortion we kept the plates in a well levelled tank and did not touch them from the beginning of the soaking stage until they were removed completely dried from the concentrated alcohol bath. We found the distortions in these emulsions reasonable (~ 30 Covans in the larger and ~ 80 Covans in the smaller of the two blocks).

(*e*) *Experimental Details of Alignment*

Two microscopes were placed close to each other. One was a travelling microscope and the other an ordinary stationary microscope with a moveable stage. Two different points on the plate could be viewed simultaneously. The microscope slides are pasted onto plastic frames in the same manner as described previously. For pasting we used a thin celluloid solution in 80% acetone and 20% amyl acetate. This solution takes about one minute to dry which is adequate for making accurate adjustments. The plate is moved until the cross of two Polonium lines appear in the center of the "stationary microscope" field. The travelling microscope is then adjusted until another Polonium line appears in the center of its field. The next plate is then glued on its frame in such a position that the identical configuration appears in the two microscopes when viewing corresponding surfaces.

The accuracy obtained by this procedure is about 5μ. An additional $\sim 5\mu$ error arises from the elastic deformation of the plastic frame when placed in the stage holder. The resulting $5–10\mu$ accuracy applies only to those points which were used for plate alignment. Other points on the plate will be displaced with respect to each other because of distortion and possible stretching of sheets at the time when they were rolled on to glass plates. We find that except near the processed edge or near a bubble, the average error is between 20 and 30μ, and, with very few exceptions, it is less than 50μ for all points on the plate.

IV. Acknowledgements

We want to express thanks to all of our colleagues who participated in the balloon flights, the processing and the aligning operations which altogether required more than six months of combined effort.

We are particularly indebted to Mrs. A. Krishnan for taking charge of making the nylon grids, and to Mr. Rama who did much of the alignment work.

Many other persons helped us in various ways during the balloon flights especially in the problems of tracking and recovery. Our particular thanks are due to Dr. K. S. Krishnan and Dr. K. N. Mathur of the National Physical Laboratory; Group Captain H. S. Moolgavkar, Chief of the Operational Command of the Indian Air Force; Dr. P. R. Krishna Rao and Dr. L. S. Mathur of the Indian Meteorological Department; Mr. M. P. Koirala, Prime Minister of Nepal; Dr. V. Sarabhai and Professor K. R. Ramanathan of the Physical Research Laboratory at Ahmedabad.

INTERMEDIATE LAYERS OF IONISATION BETWEEN THE E AND F_1 LAYERS OF THE IONOSPHERE OVER AHMEDABAD (23° N, 72°·6 E)

By R. G. Rastogi

(Physical Research Laboratory, Ahmedabad)

Received September 9, 1954

(Communicated by Dr. K. R. Ramanathan)

Introduction

The existence of an ionised layer intermediate between the two main layers E and F_1 was first reported by Schafer and Goodall,[1] and shortly afterwards by Appleton,[2] and by Ratcliffe and White.[3] Similar observations were later reported by Gilliland,[4] and by Lung.[5] This intermediate layer, now called E_2, was generally observed during morning and evening hours[2] and mainly in the winter months.[5] A more detailed study of this layer has been made by Becker and Dieminger.[6, 8] They found that the E_2 layer occurred regularly; it had an average virtual height of 130–140 km. The layer also showed evidence of magneto-ionic splitting. Becker and Dieminger suggested that the ionisation of the layer might be due either to neutral corpuscles or to a small range of frequencies of ultra-violet radiation from the sun. Commission III of the U.R.S.I. on 'Ionosphere and Propagation' in their recommendation to the 1948 General Assembly at Stockholm made the following remark,[7] "In the event that clear stratification is evident within the regular E layer, and a second critical frequency is observed, it is increasingly common practice to refer to the upper critical frequencies as f_0E_2 and f_xE_2 and the minimum virtual height as $h'E_2$." Becker and Dieminger in their second paper have concluded that the E_2 layer should be considered as a continuous thin homogeneous layer.

Leiv Harang[9] in 1937 noted two stratifications between the E and F_1 layers. Soon after the ionospheric station at Ahmedabad was established in 1953, it was noticed that between the E and F_1 layers, there were often two regular ionisation steps indicating discrete ionised layers. An example of such an occurrence is shown in Fig. 1.

Symbols used.—Throughout this paper, we shall indicate the normal E layer simply as the E layer, and the two intermediate layers as E_1 and E_2,

the upper one being called E_2. The ordinary wave critical frequencies for the E, E_1, E_2 and F_1 layers will be indicated by f_0E, f_0E_1, f_0E_2 and f_0F_1 and the minimum virtual heights by $h'E$, $h'E_1$, $h'E_2$ and $h'F_1$. This would be consistent with the recommendations of U.R.S.I.[7]

Frequencies of Occurrence of the Layers

E_1 and E_2 layers are most clearly seen shortly after sunrise. During evening hours they are less clear owing to interference and absorption. They are least clear during the noon hours, presumably due to absorption. Fig. 2 gives the percentage frequencies of occasions on which these layers could be observed in February, March and April 1953.

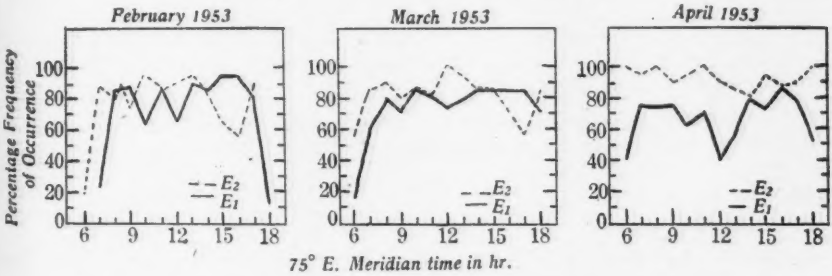

Fig. 2. Frequencies of occurrence of the E_1 and E_2 Layers during February, March and April 1953.

Critical Frequencies of the Layers

Both E_1 and E_2 layers show magnetic splitting similar to the normal E layer. The extraordinary components of E_1 and E_2 are recorded as weak reflections except in the morning and evening hours. Fig. 3 shows a P'-*f* record in which the extraordinary components are clearly visible.

The observed critical frequencies indicate that the E_1 and E_2 layers are almost as regular as the main layers E and F_1. Moreover the scatter of the values of f_0E_1 and f_0E_2 is of the same order of magnitude as the scatter of f_0E and f_0F_1. On the average, f_0E_1 is only slightly larger (0·2 Mc/s) than the corresponding f_0E, and the average difference between f_0E_2 and f_0E_1 is 0·6 Mc/s.

Table 1 gives the median values of the critical frequencies of the layers E, E_1, E_2 and F_1 for the months of February, March and April 1953. The values are plotted in Fig. 4. The figure shows that similar to the normal layers, E_1 and E_2 also follow the sun's altitude.

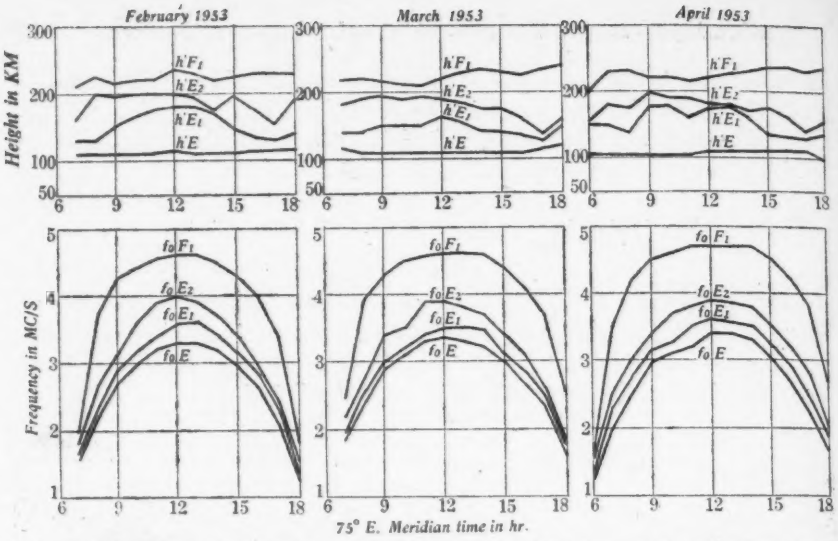

FIG. 4. Curves showing the median values of the critical frequencies and virtual heights of E, E_1, E_2 and F_1 layers during the months of February, March and April 1953.

TABLE I

Monthly median values of the critical frequencies (in Mc/s) of E, E_1, E_2 and F_1 layers during the months of February, March and April 1953

Hours 75° E.M.T.	February				March				April			
	f_0E	f_0E_1	f_0E_2	f_0F_1	f_0E	f_0E_1	f_0E_2	f_0F_1	f_0E	f_0E_1	f_0E_2	f_0F_1
6	..	..	1·15	..	..	..	1·1	..	1·25	1·3	1·6	..
7	1·6	1·65	1·8	1·95	1·9	1·95	2·2	2·45	2·0	2·3	2·5	3·5
8	2·2	2·35	2·65	3·7	2·4	2·55	2·75	3·9	2·5	2·75	3·05	4·2
9	2·7	2·9	3·1	4·25	2·9	3·0	3·4	4·3	3·0	3·25	3·45	4·5
10	3·0	3·15	3·6	4·4	3·1	3·2	3·5	4·5	3·1	3·25	3·7	4·6
11	3·1	3·4	3·9	4·55	3·3	3·4	3·9	4·55	3·2	3·5	3·8	4·7
12	3·2	3·6	4·0	4·6	3·35	3·5	3·9	4·6	3·4	3·6	3·9	4·7
13	3·2	3·6	3·9	4·6	3·3	3·5	3·8	4·6	3·4	3·55	3·85	4·7
14	3·1	3·4	3·7	4·5	3·2	3·45	3·7	4·6	3·3	3·5	3·8	4·7
15	2·95	3·15	3·4	4·3	3·0	3·1	3·4	4·4	3·0	3·2	3·5	4·5
16	2·65	2·85	2·95	4·0	2·65	2·85	3·1	4·1	2·65	2·9	3·15	4·2
17	2·0	2·25	2·4	3·4	2·3	2·55	2·6	3·7	2·2	2·4	2·8	3·8
18	..	..	1·55	..	..	1·6	1·8	2·5	1·7	1·9	2·0	2·7

The critical frequencies of these intermediate layers obey approximately the law

$$f_0 = k \cos^n Z,$$

where Z is the sun's zenith distance and k and n are constants. Fig. 5 shows the graph of the critical frequencies of E, E_1, E_2 and F_1 layers against cos Z for the month of March 1953. The values of k and n are given in Table II.

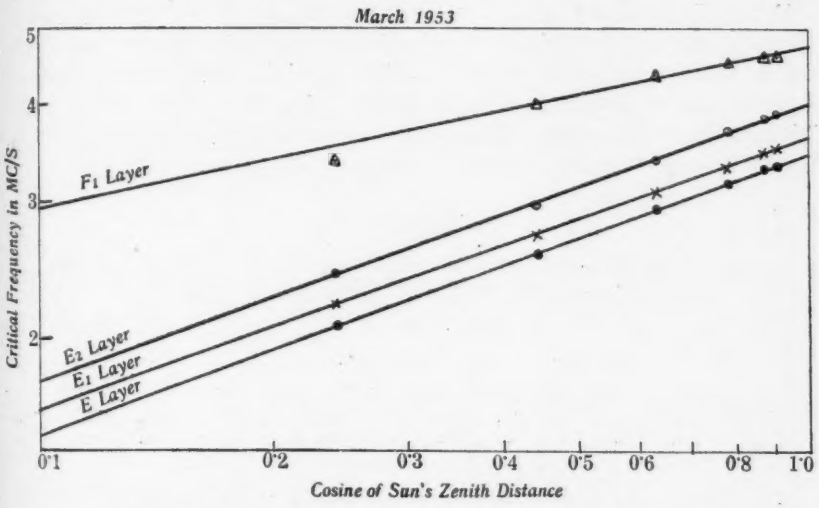

FIG. 5. Graph of critical frequency *versus* cos Z for the layers E, E_1, E_2 and F_1 during the month of March 1953.

TABLE II

Values of k *and* n *for E, E_1, E_2 and F_1 layers during the months of February, March and April* 1953

Layer	February		March		April	
	k	*n*	*k*	*n*	*k*	*n*
E ..	3·5	0·35	3·5	0·37	3·4	0·41
E_1 ..	3·9	0·38	3·6	0·35	3·6	0·38
E_2 ..	4·3	0·41	4·1	0·39	3·9	0·36
F_1 ..	4·8	0·22	4·7	0·21	4·8	0·20

If the ionisation followed a simple Chapman Law, the constant n would be 0·25, whereas the observed values are near 0·38 for E, E_1 and E_2 layers and near 0·21 for the F_1 layer.

VIRTUAL HEIGHTS OF THE LAYERS

As regards the heights of these layers, the individual observations of the virtual height are rather widely scattered. The observed virtual heights of E_1 and E_2 layers are usually considerably greater than the true heights of reflection due to the proximity of the critical frequencies of the underlying layers. Consequently the values of $h'E_1$ and $h'E_2$ show large variations depending upon the nearness of the critical frequencies of the lower layers. Table III gives the median values of the minimum virtual heights of E, E_1, E_2 and F_1 layers for the months of February, March and April 1953.

TABLE III

Median values of the minimum virtual heights of E, E_1, E_2 and F_1 layers during the months of February, March and April 1953

Hours 75° E.M.T.	February				March				April			
	$h'E$ km.	$h'E_1$ km.	$h'E_2$ km.	$h'F_1$ km.	$h'E$ km.	$h'E_1$ km.	$h'E_2$ km.	$h'F_1$ km.	$h'E$ km.	$h'E_1$ km.	$h'E_2$ km.	$h'F_1$ km.
6	..	..	160	..	..	..	170	..	105	150	155	..
7	110	130	160	210	115	140	180	220	105	150	180	230
8	110	130	200	225	110	140	190	220	105	138	175	230
9	110	150	195	215	110	150	195	215	105	175	200	220
10	110	165	200	220	110	150	190	210	105	185	190	220
11	110	175	200	220	110	150	195	210	105	160	190	215
12	115	180	200	235	110	165	190	220	110	180	175	220
13	110	180	195	230	110	155	185	230	110	180	180	225
14	110	170	175	220	110	140	175	233	110	160	170	230
15	110	145	195	225	110	140	175	230	110	135	175	235
16	115	135	175	230	110	135	160	225	110	130	160	235
17	115	130	155	230	115	125	135	235	110	130	140	230
18	..	..	190	..	..	150	160	240	100	130	150	235

True Heights of the Layers

The true height of the ionisation maximum of a layer can be determined with the help of Booker and Seaton's formula[10]

$$h' = h_m + \mathrm{T}\,\phi\,(f/f_c)$$

where h' is the virtual height of reflection for a wave of frequency f, h_m the height of ionisation maximum, T the semi-thickness of the layer and ϕ is a function defined by

$$\phi\left(\frac{f}{f_c}\right) = \frac{1}{2}\,\frac{f}{f_c}\log_e\left|\frac{f_c+f}{f_c-f}\right| - 1$$

where f_c is the critical frequency of the layer. If another layer lies just above the height of maximum ionisation of the lower layer then the group retardation of a wave ($f > f_c$) penetrating the lower layer is given by

$$\Delta h' = \mathrm{T}\,\phi\left(\frac{f}{f_c}\right)$$

But if the upper layer overlaps the lower layer below its ionisation maximum then the group retardation by the lower layer is given by a formula given by Ratcliffe.[11]

$$\Delta h' = \mathrm{T}\,(f/f_c)\log_e\left\{\frac{1+f/f_c}{\sqrt{1-(f_B/f_c)^2}+\sqrt{(f/f_c)^2-(f_B/f_c)^2}}\right\}$$

where f_c is the critical frequency of the lower layer and f_B is the frequency at which the reflections start from the upper layer. Thus h_m and T of a layer can be determined by fitting the observed P'–f curve with the standard P'–f curves drawn on a transparent sheet according to the above formula [Ratcliffe's method[11]]. The values of h' are plotted against [Appleton and Beynon's method[12]] and the slope of the straight line passing through the points gives T, and its intercept on the h' axis gives h_m.

Such a determination of true height is often not possible for these intermediate layers due to the very short trace of P'–f curve which is visible, or the frequent overlapping of the layers, or the presence of scattered E or sporadic E reflections. The heights of these layers on a number of days were determined by Ratcliffe's method. The values were verified by Appleton and Beynon's method. Table IV gives the results of such determination from a few clear P'–f records.

The true heights of E_2 layer were calculated to which the above method could be applied, from all records of March 1953 and Table V gives the mean values of the true heights of E and E_2 layers during March 1953.

TABLE IV

Virtual and true heights of E, E_1 and E_2 layers on some individual days

Date (1953)	Time 75° E.M.T. hr.	E Layer			E_1 Layer			E_2 Layer		
		h' (km.)	h_m (km.)	T (km.)	h' (km.)	h_m (km.)	T (km.)	h' (km.)	h_m (km)	T (km.)
12th February ..	0800	100	112	5	128	125	18	155	145	<5
13th February ..	0800	115	113	10	130	118	22	150	130	8
2nd March ..	1600	110	114	10	132	120	18	150	140	<5
12th March ..	1100	115	106	25	155	120	10	140	135	<5
1st April ..	0800	120	118	20	152	122	10	170	155	<5
16th April ..	0700	112	110	12	130	126	22	160	150	<5

TABLE V

Mean true heights of ionisation maximum of normal E and E_2 layers during March 1953

Time 75° E.M.T. Hr.	E Layer			E_2 Layer		
	No. of occasions	h_m (km.)	T (km.)	No. of occasions	h_m (km.)	T (km.)
06	..	..	..	5	160	15
07	8	116	12	7	159	15
08	8	113	10	4	142	15
09	6	107	11	6	155	10
10	8	109	22	7	134	5
11	7	110	24	11	148	< 5
12	11	112	18	7	142	< 5
13	11	112	20	9	137	< 5
14	9	112	26	14	139	< 5
15	15	116	20	14	141	< 5
16	18	116	17	15	140	< 5
17	10	120	15	14	127	< 5
18	..	..	..	8	135	< 5

On the average, the E_2 layer occurs at a height of about 140 km.; it is a very sharp layer having a semi-thickness less than 5 km., while normal E occurs at the height of about 115 km. and has an average semi-thickness of 18 km. E_1 occurs at the height of 120 to 130 km. and is of about the same thickness as the E layer.

After sunrise, the E_2 layer is the one to appear first and E_1 and E layers develop later. From the observations taken at intervals of 5 min. in the morning hours during another season, it was found that E_2 layer developed approximately 10–20 min. before the appearance of the E layer. The F_1 layer becomes distinguishable from the general F layer only about an hour after the appearance of the E_2 layer. It appears that as the sun's altitude increases and the sun's rays illuminate the lower strata of the atmosphere, the ionospheric layers develop successively. Fig. 6 illustrates the development of these layers on 11th February 1953.

There have recently been a few determinations of the electron concentrations in the ionosphere with the aid of rockets. Seddon[13] obtained on 29th September 1949 a value of electron density for the E layer $1{\cdot}6\times10^5$ electrons per c.c. at a height of 107 km., and for the E_2 layer $2{\cdot}2\times10^5$ electrons per c.c. at 142 km. The usual ionospheric P′–*f* record obtained during the rocket firing showed the virtual height of the E_2 layer to be 215 km. In the diagram given by Seddon there is also a secondary maximum of electron concentration at about 120 km. The data obtained by J. R. Lien and collaborators[14] on 26th June 1953 gave for the normal E layer $1{\cdot}3\times10^5$ electrons per cm.^{3} at a height of 110 km. and for the E_2 layer 2×10^5 electrons per cm.^{3} at a height exceeding 130 km. The diagram given by the authors shows a third intermediate maximum at 120 km. with electron density lower than that of either the normal E layer or of the E_2 layer. Bering's[15] data obtained on 15th Dec. 1952 gave for the normal E layer a charge density of $1{\cdot}0\times10^5$ per cm.^{3} at a height of 103 km. The next higher layer appeared at 123 km. with a charge density nearly the same as that of the normal E layer and a third maximum at 156 km. with $1{\cdot}4\times10^5$ per cm.^{3} The electron density maxima between the main layers E and F_1 as obtained by rocket data thus correspond reasonably well with the two layers E_1 and E_2 regularly observed at Ahmedabad.

It seems to be of importance to maintain systematic records of the appearance, critical frequencies and other characteristics of the E_2 and E_1 layers. A more extended study of the phenomenon has been undertaken by the author.

SUMMARY

Between the main layers E and F_1 of the ionosphere over Ahmedabad, two intermediate layers occur regularly having virtual heights of 125 and 140 km. They also show the characteristic magneto-ionic splitting. The critical frequencies of these layers follow the position of the sun according to the law $f_0 = k \cos^n Z$, n neing near about 0·38. Minimum virtual heights of these layers have been shown to be very misleading due to the proximity of the lower layers. The true height and the thickness have been determined for some cases. The true heights of these layers correspond well with the heights of ionisation maxima in the ionosphere determined with the aid of rockets.

ACKNOWLEDGEMENT

I am very grateful to Dr. K. R. Ramanathan, for his continuous encouragement and kind guidance in the work, and to Dr. U. D. Desai for his valuable help during the installation of the ionospheric station. The Council of Scientific and Industrial Research (India), is supporting the Ionospheric Station with financial assistance.

REFERENCES

1. Schafer, J. P. and Goodall, W. M. — *Nature*, 1933, **131**, 804.
2. Appleton, E. V. .. — *Ibid.*, 1933, **131**, 872.
3. Ratcliffe, J. A. and White, E. L. C. — *Ibid.*, 1933, **131**, 873.
4. Gilliland, T. R. .. — *Proc. Inst. Radio Engr.*, 1935, **23**, 1076.
5. Lung, H. L. .. — *U.R.S.I. Proc. Eighth General Assembly*, held in Stockholm, 1949, 250.
6. Becker, W. and Dieminger, W. — *Naturwissenschaften*, 1950, **37**, 90.
7. *U.R.S.I. Information Bulletin on Terminology and Symbols*, Commission III on Ionosphere and Propagation, 1949, 10.
8. Becker, W. and Dieminger, W. — "U.R.S.I. Mixed Commission on Ionosphere," *Proc. Second Meeting*, held in Brussels, 1950, 126.
9. Harang, L. .. — *Terr. Mag. and Atmos. Elect.*, 1937, **42**, 68.
10. Booker, H. G. and Seaton, S. L. — *Phys. Rev.*, 1940, **57**, 87.
11. Ratcliffe, J. A. .. — *J. Geophy. Res.*, 1951, **56**, 463.
12. Appleton, E. V. and Beynon, W. S. G. — *Proc. Phys. Soc.*, 1940, **52**, 518.
13. Seddon, J. C. .. — *J. Geophy. Res.*, 1953, **58**, 323.
14. Lien, J. R., Marcou, R. J., Ulwick, J. C., Aarons, J. and Mc Morrow, D. R. — *Rocket Exploration of the Upper Atmosphere*, Pergamon Press Ltd., London, 1954, 232.
15. Bering, W. W. .. — *Ibid.*, 1954, 272.

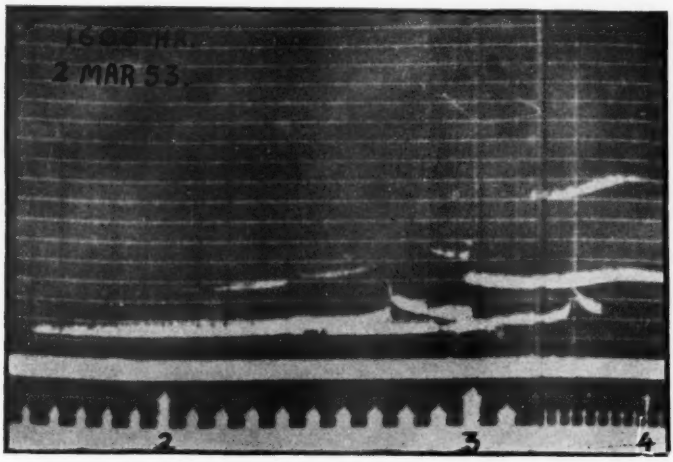

FIG. 1

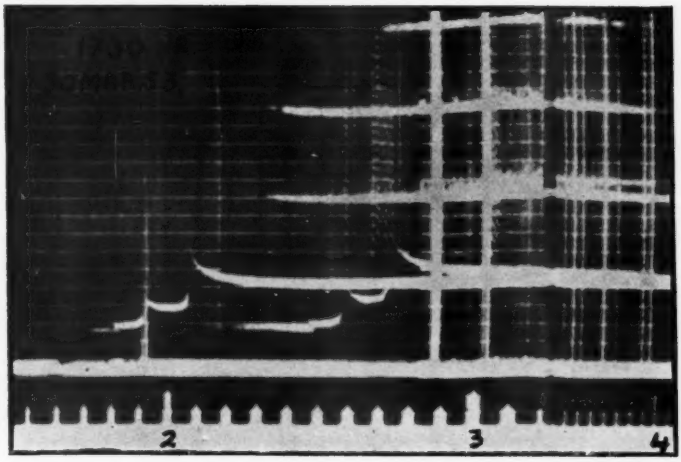

FIG. 3

FIG. 1. P′-*f* record taken at 1600 hr. 75° East Meridian Time on 2nd March 1953. Two intermediate layers between main E and F_1 layers can be clearly seen, particularly in the second curve.

FIG. 3. P′-*f* record taken at 1730 hr. 75° East Meridian Time on 30th March 1953. Ordinary as well as extraordinary components of E, E_1 and E_2 layers are clearly visible.

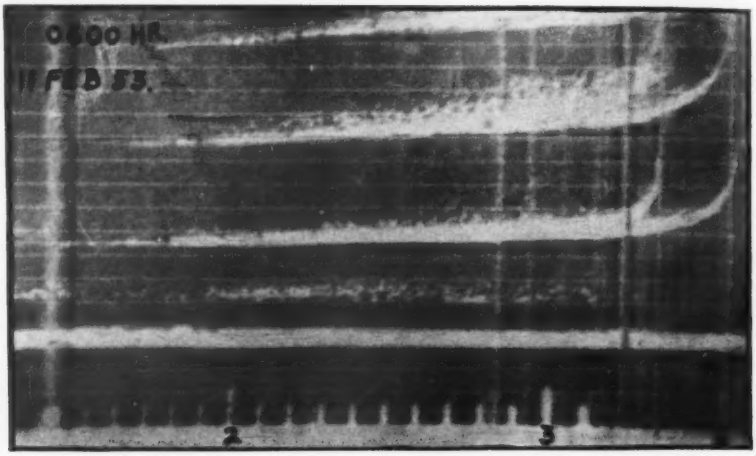

FIG. 6*a*

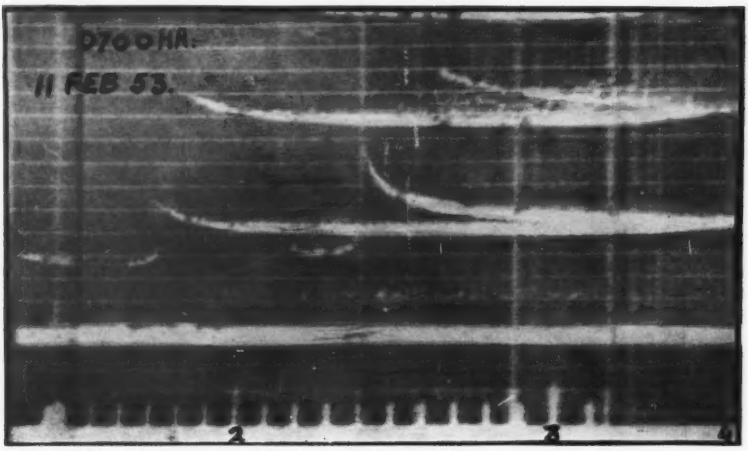

FIG. 6*b*

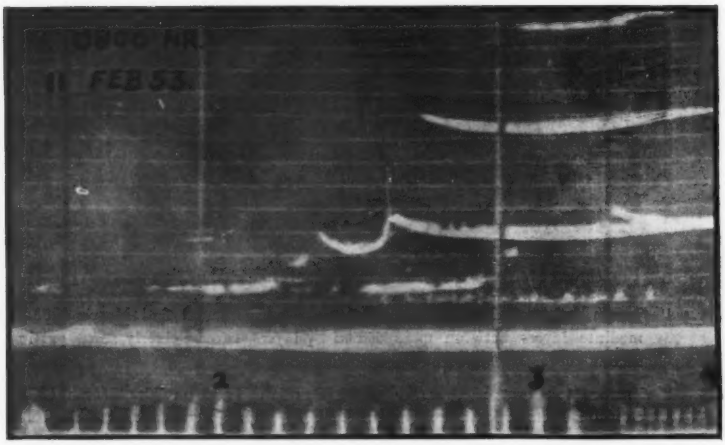

FIG. 6*c*

FIGS. 6*a*, 6*b*, 6*c*. The successive development of the ionospheric layers in the morning hours on 11th February 1953.

PHOTOELASTIC STUDIES OF OPTICALLY ACTIVE CRYSTALS

$NaClO_3$ and $NaBrO_3$

By T. S. Narasimhamurty

(From the Physical Laboratories, Osmania University, Hyderabad)

Received March 8, 1954

(Communicated by Prof. S. Bhagavantam)

1. Introduction

Crystals of $NaClO_3$ and $NaBrO_3$ belong to the crystal class T and exhibit optical activity. Determination of their photoelastic constants is of interest. The usual methods of studying optically inactive substances cannot be employed in such cases for obvious reasons; and special techniques have been employed by previous investigators in the case of $NaClO_3$ (Ramachandran and Chandrasekharan, 1951). In the present investigation, an optical method using the Rayleigh Compensator has been employed. It is very sensitive, being capable of measuring a birefringence of the order of $1/500\,\lambda$. The sensitiveness, which can be varied at will, is independent of the magnitude of the birefringence to be measured and remains uniform throughout the range of measurement. Such measurements give directly the values of $(q_{11}-q_{12})$, $(q_{11}-q_{13})$ and q_{44}.

From a study of the state of polarisation of the ultrasonic diffraction patterns (Mueller, 1938), the ratios of the elasto-optic constants have been determined by Burstein, Smith and Henvis (1950) for cubic crystals belonging to the classes T_d, O and O_h and by Vedam (1950) for glasses. Both the theory of Mueller and the experimental technique have been modified by Vedam and Ramachandran (1951), to suit the case of sodium chlorate which is optically active. This modified method has been employed in this investigation as well for determining the ratios of the elasto-optic constants. Hence the absolute values of the several constants are calculated.

2. The Rayleigh Compensator

A plane sheet of glass ABCD (Fig. 1 *a*), bent into the form A′B′C′D′ (Fig. 1 *b*) constitutes the Rayleigh Compensator (Rayleigh, 1902; Ramanadham, 1929). When the glass plate is strained as indicated, the region

along NN′ undergoes no strain and hence forms the neutral region. Portions of the plate above NN′ experience a tensile stress and portions below NN′ experience a compressional stress. The result is that the upper half of the plate behaves as a positive uniaxial crystal and the lower part as a negative uniaxial crystal, the two being separated by a neutral band. When such a plate is viewed through crossed Nicols, light is completely extinguished

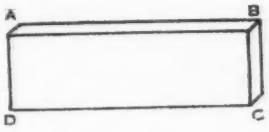

FIG. 1 *a*

FIG. 1 *b*

at the neutral region only; but appears over the rest of the field. Now if a birefringent medium G (*e.g.*, a longitudinally compressed glass block, Fig. 2 *a*) is placed between the polariser and the Rayleigh compensator, the dark band shifts upward or downward depending upon the sign of birefringence of the medium G, with respect to that of the Rayleigh Compensator. The shift of the dark band can be detected by a low power telescope. Further, if the telescope is provided with a finely divided scale in the place of cross wires, the shift can be measured in terms of scale divisions and it can be used as a measure of birefringence, after calibration. The sign of birefringence of the specimen can be determined unambiguously, by comparing the direction of the shift for the specimen with that for glass.

If the specimen has optical activity but no birefringence, light is restored in the entire field of view; and the dark band NN′ reappears in the field of view of the telescope when the analyser is rotated through the appropriate angle. The band reappears now exactly at the former scale division. Thus the birefringence and optical activity could be studied.

Now to experiment with an optically active medium, the specimen is placed between the Rayleigh Compensator and the analyser; the analyser is rotated until the neutral dark band reappears. The specimen is then compressed lengthwise. The band then shifts upward or downward depending upon its sign of birefringence. If in addition to the stress birefringence, the optical activity of the medium itself changes with stress, the dark band becomes diffuse and tends to disappear; it can be seen again by rotating the analyser, through the necessary angle. Thus change in optical activity alone will render it diffuse but produces no shift while birefringence alone will produce the shift but the band remains dark.

3. The Experimental Set-up

The compressing arrangement is shown in Fig. 2 *a*. Since the Rayleigh Compensator could detect birefringence of the order of even $\frac{1}{500}$ λ, no lever arrangement was found necessary. The beam BB carrying the loads W, W at either end, rests on the specimen. Paper and rubber spacers were used to render the stress uniform on the crystal.

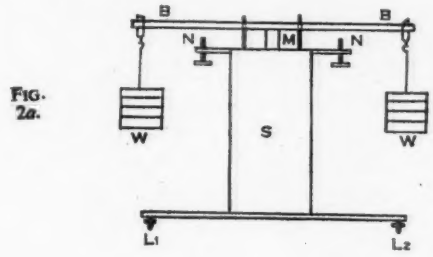

Fig. 2*a*.

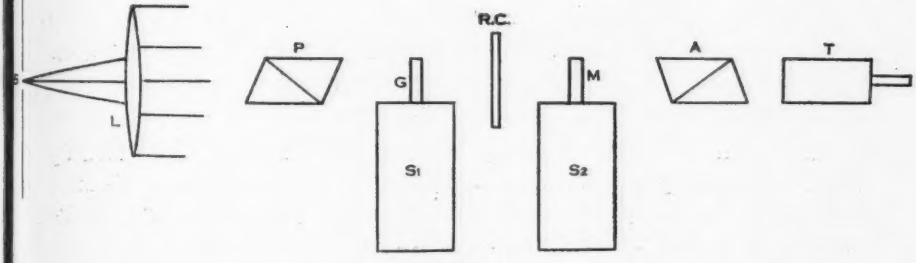

Fig. 2 *b*

Two such compressing arrangements S_1, S_2 (Fig. 2 *b*) have been set up, one on either side of the Rayleigh Compensator R.C. The polariser P is set at 45° with the vertical.

A glass prism G (1 cm. × 0·75 cm. × 0·45 cm.) is first stressed under a known load and the consequent birefringence produced is determined with a Babinet compensator; the amount of birefringence (in terms of the light source used) is calculated for a load of 1,000 gm. In the present investigation for a load of 1,000 gm. the path difference = 53·7 Å when the prism is stressed lengthwise and direction of observation is parallel to the smallest dimension. The glass prism G is then used as the standard with which the birefringence is compared.

The glass prism G which is of isotropic medium develops only birefringence under linear stress but no rotation, whereas the crystal prism M which is initially optically active becomes also birefringent under linear stress and hence there is an *apparent* rotation of the axes of birefringence (Ramaseshan, 1951). For this reason the specimen M (*i.e.*, of sodium chlorate or sodium bromate) is mounted on S_2 and the glass prism G on S_1. The dark band will now be seen when the analyser is rotated through an angle equal to the optical rotation by M. M is then stressed by a load of say 2,000 gm. (*i.e.*, 1,000 gm. at either end) and the shift of the band is noted in the field of view of the telescope. M is then unloaded and G is loaded suitably so that the dark band showed the *same displacement* as for the medium M. Hence the birefringence produced is the same for both. From this the corresponding piezo-optic constants of the medium could be calculated. It may be mentioned here that the crystal prism must be very well polished so that the dark band may be seen clearly. A freshly polished prism is to be preferred. Further, the levelling of the bases and of the seat of the prism must be fairly good so that the distribution of pressure on the prism is uniform. The non-uniformity of pressure is revealed by the fact that the dark band no longer remains straight and horizontal but gets inclined and distorted. Lastly, with so sensitive an apparatus as the Rayleigh Compensator, the slightest imperfections in the crystals render them unfit for the work since the whole field of view is then covered by a cobweb pattern of the neutral band.

Measurements of the birefringence have been made for both $NaClO_3$ and $NaBrO_3$ using the Rayleigh Compensator; and the results obtained have been checked up using the elliptic analyser (previously employed by Ramachandran and Chandrasekharan, 1951).

4. DIMENSIONS OF THE PRISMS EMPLOYED

TABLE I *a*

Sodium Chlorate

	Sense of rotation	Length		Breadth		Thickness	
		‖ to	mm.	‖ to	mm.	‖ to	mm.
1	L	[001]	10·53	[010]	4·70	[100]	4·50
2	L	„	14·13	„	7·87	„	6·54
3	L	[$\bar{1}$10]	11·63	[011]	6·16	[100]	5·20
4	L	[111]	13·12	[$\bar{2}$11]	9·18	[0$\bar{1}$1]	7·45

TABLE I *b*

Sodium Bromate

	Sense of rotation	Length		Breadth		Thickness	
		‖ to	mm.	‖ to	mm.	‖ to	mm.
1	R	[001]	8·74	[010]	3·17	[100]	3·88
2	R	„	7·35	„	3·26	„	3·64
3	R	[110]	10·40	[1$\bar{1}$0]	5·15	[001]	4·12
4	R	[111]	7·88	[1$\bar{1}$0]	4·87	[11$\bar{2}$]	4·57

5. RESULTS FOR $NaClO_3$

TABLE II

Measurements with Rayleigh Compensator for Prism No. 1

Direction of stress on $NaClO_3$	Direction of observation in $NaClO_3$	Load on $NaClO_3$ in kgm.	Load on glass in kgm.	Load on $NaClO_3$ / Load on glass
[001]	[100]	3·25	2·00	1·625
		4·75	3·00	1·583
		6·25	4·00	1·563
				mean: 1·59
[001]	[010]	1·75	2·00	0·875
		2·75	3·00	0·917
		3·50	4·00	0·875
				mean: 0·89

The mean of the values in the last column gives the stress on $NaClO_3$ to produce a path difference of 53·7 Å which is the path difference produced in the glass for a load of 1 kgm. Hence the appropriate $f(q)$ of $NaClO_3$ is determined.

The values of the several constants of $NaClO_3$ used in the calculation are as follows:—

Refractive Index for Na yellow light: 1·514.

$c_{11} = 5{\cdot}00 \times 10^{11}$; $c_{12} = 1{\cdot}47 \times 10^{11}$; $c_{44} = 1{\cdot}18 \times 10^{11}$ dynes/sq. cm.

(*a*) From the observations in Table II, we obtain $q_{11}-q_{12}=-2\cdot35\times10^{-13}$ and $q_{11}-q_{13}=-1\cdot45\times10^{-13}$.

(*b*) The piezo-optic constants have also been determined using the elliptic analyser and the mean values of $(q_{11}-q_{12})$, $(q_{11}-q_{13})$ and q_{44} have been collected below:

$$q_{11}-q_{12}=-2\cdot43\times10^{-13};\quad q_{11}-q_{13}=-1\cdot38\times10^{-13};$$

$$q_{44}=-1\cdot68\times10^{-13}.$$

(*c*) Elasto-optic constants:

From a study of the polarisation of the ultrasonic diffraction pattern (Mueller, 1938) of $NaClO_3$ prisms Nos. (1), (2) and (3), the values obtained are given below. In the calculation of the results, the observed values have been extrapolated to zero ultrasonic amplitude (Vedam, 1950) and allowance has been made for the optical activity of the crystal (Vedam and Ramachandran, 1951).

$$\frac{p_{12}}{p_{11}}=\tan(45^\circ+11^\circ)=1\cdot48\ ;\ \frac{p_{13}}{p_{11}}=\tan(45^\circ+7^\circ)=1\cdot28$$

$$\frac{2p_{11}+p_{12}+p_{13}-4p_{44}}{2p_{11}+p_{12}+p_{13}+4p_{44}}=\tan(45^\circ+6^\circ)=1\cdot13.$$

Thus the complete set of photoelastic constants for $NaClO_3$ are:

$$p_{11}=0\cdot162;\ p_{12}=0\cdot24;\ p_{13}=0\cdot20;\ p_{44}=-0\cdot0198$$

$$q_{11}=1\cdot43\times10^{-13};\ q_{12}=3\cdot78\times10^{-13};\ q_{13}=2\cdot88\times10^{-13};$$

$$q_{44}=-1\cdot68\times10^{-13}\text{ in units of cm.}^2\text{ dyne}^{-1}.$$

These results agree fairly well with the results obtained earlier by Ramachandran and Chandrasekharan (1951) quoted below:

$$p_{11}=0\cdot173;\ p_{12}=0\cdot258;\ p_{13}=0\cdot223;\ p_{44}=-0\cdot0187$$

$$q_{11}=1\cdot48\times10^{-13};\ q_{12}=3\cdot88\times10^{-13};\ q_{13}=2\cdot89\times10^{-13}$$

$$q_{44}=-1\cdot58\times10^{-13}\text{ in units of cm.}^2\text{ dyne}^{-1}.$$

The present method could therefore be considered to be accurate for determining small birefringences of the order now investigated and it has been used for determining the photoelastic constants of sodium bromate.

6. Results for $NaBrO_3$

TABLE III

Measurements with Rayleigh Compensator for Prism No. 2

Direction of stress	Direction of observation	Load (in kgm.) on $NaBrO_3$	Load (in kgm.) on glass	Load on $NaBrO_3$ / Load on glass
[001]	[100]	1·80	2·00	0·90
		2·75	3·00	0·917
		3·55	4·00	0·888
				mean: 0·90
[001]	[010]	2·50	2·00	1·25
		3·50	3·00	1·17
		4·75	4·00	1·19
				mean: 1·20

The mean of the values in the last column gives the stress on $NaBrO_3$ to produce a path difference of 53·7 Å which is the path difference produced in the standard glass prism for a load of one kilogram. Hence the value of the appropriate $f(q)$ of $NaBrO_3$ is determined.

The values of the several constants of $NaBrO_3$ used in the calculations are as follows:—

Refractive index of $NaBrO_3$ for Na yellow light: 1·594 (I.C.T.)
$c_{11} = 5{\cdot}45 \times 10^{11}$; $c_{12} = 1{\cdot}92 \times 10^{11}$; $c_{44} = 1{\cdot}50 \times 10^{11}$ dynes/sq. cm.
(Sundara Rao, 1948).

From the observations, we obtain $q_{11} - q_{12} = -0{\cdot}98 \times 10^{-13}$;

$q_{11} - q_{13} = -0{\cdot}82 \times 10^{-13}$.

The values of the above piezo-optic constants have been determined using the elliptic analyser for the same orientation of the $NaBrO_3$ prism. The results are given in Table IV (for an explanation of the symbols, see Ramachandran and Chandrasekharan, 1951).

These gave the values $q_{11} - q_{12} = -1{\cdot}02 \times 10^{-13}$ and

$q_{11} - q_{13} = -0{\cdot}85 \times 10^{-13}$.

Similarly all the other piezo-optic constants have been determined for the several prisms using both the Rayleigh Compensator and the elliptic analyser and the mean values are:

$q_{11} - q_{12} = -0{\cdot}95 \times 10^{-13}$; $q_{11} - q_{13} = -0{\cdot}80 \times 10^{-13}$;

$q_{44} = -0{\cdot}93 \times 10^{-13}$ in units of cm.^{2} dyne^{-1}.

TABLE IV

Load in kgm.	Observation along [100]			Observation along [010]		
	ξ	$\delta/2\rho$ $=\tan(90-2\xi)$	$\delta/2\rho$ per kgm.	ξ	$\delta/2\rho$ $=\tan(90-2\xi)$	$\delta/2\rho$ per kgm.
0	45	..	..	45	..	..
$0{\cdot}75\times5$	27	0·727	0·97	24	0·900	1·20
$1{\cdot}25\times5$	20	1·192	0·95	18	1·376	1·10
$1{\cdot}75\times5$	14	1·881	1·08	12	2·246	1·14
$2{\cdot}00\times5$	12	2·246	1·12	9	3·078	1·54

Studies on the state of polarisation when ultrasonic beam is propagated along the cube axes and along the face-diagonal have given the following values (after allowing for the finite amplitudes of the ultrasonic beam and for the optical activity of the sodium bromate):

$$p_{12}/p_{11} = \tan(45^\circ + 4{\cdot}5^\circ);\ p_{13}/p_{11} = \tan(45^\circ + 4^\circ)$$

and
$$\frac{2p_{11} + p_{12} + p_{13} - 4p_{44}}{2p_{11} + p_{12} + p_{13} + 4p_{44}} = \tan(45^\circ + 4^\circ)$$

The experimental observation that almost the same value has been obtained for both p_{12}/p_{11} and p_{13}/p_{11} indicates clearly that one cannot very much rely on the small difference of $0{\cdot}5^\circ$ observed for the two ratios p_{12}/p_{11} and p_{13}/p_{11}. Hence in calculating the absolute values, it has been felt desirable to ignore the values for p_{12}/p_{11} and p_{13}/p_{11}.

The ratio $\dfrac{2p_{11} + p_{12} + p_{13} - 4p_{44}}{2p_{11} + p_{12} + p_{13} + 4p_{44}} = \tan 49^\circ = 1{\cdot}15$

which contains all the four coefficients, has been taken into consideration for calculating the absolute values of p's and q's.

Thus the complete set of photo-elastic constants of $NaBrO_3$ are:

$p_{11} = 0{\cdot}185;\ p_{12} = 0{\cdot}0218;\ p_{13} = 0{\cdot}213;\ p_{44} = -0{\cdot}0139.$

$q_{11} = 1{\cdot}63\times10^{-13};\ q_{12} = 2{\cdot}58\times10^{-13};\ q_{13} = 2{\cdot}45\times10^{-13};$

$q_{44} = -0{\cdot}93\times10^{-13}$ cm.^{2} dyne^{-1}.

The author's grateful thanks are due to Dr. S. Bhagavantam for his kind interest in the work.

7. Summary

Double refraction and optical activity are studied by employing the Rayleigh Compensator and the photoelastic constants of $NaClO_3$ have been redetermined, confirming the results obtained by Ramachandran and Chandrasekharan (1951). The photoelastic constants of $NaBrO_3$, another T-class crystal, have been determined for the first time, employing the Rayleigh Compensator and also the elliptic analyser previously employed by Ramachandran and Chandrasekharan for studying $NaClO_3$; and the results confirm the theoretical prediction of Bhagavantam (1942). The values for $NaBrO_3$ are as follows: $p_{11}=0\cdot185$; $p_{12}=0\cdot218$; $p_{13}=0\cdot213$; $p_{44}=-0\cdot0139$ and $q_{11}=1\cdot63\times10^{-13}$; $q_{12}=2\cdot58\times10^{-13}$; $q_{13}=2\cdot45\times10^{-13}$ $q_{44}=-0\cdot93\times10^{-13}$ (all in units of cm.^{2} dyne^{-1}).

References

1. Bhagavantam, S. .. *Proc. Ind. Acad. Sci.*, 1942, **16A**, 359.
2. Burstein, E., Smith, P. and Henvis, B. *Phys. Rev.*, 1948, **73**, 1262.
3. Mueller, H. .. *Zeit. Krist.*, 1938, **99**, 122.
4. Ramachandran, G. N. and Chandrasekharan, V. *Proc. Ind. Acad. Sci.*, 1951, **33**, 199.
5. Ramanadham, M. .. *Ind. Jour. Phy.*, 1929, **4**, 15.
6. Ramaseshan, S. .. *Proc. Ind. Acad. Sci.*, 1951, **34**, 33.
7. Rayleigh, Lord .. *Phil. Mag.*, 1902, **4**, 678.
8. Sundara Rao, R. V. G. .. *Curr. Sci.*, 1948, **18**, 204.
9. Vedam, K. .. *Proc. Ind. Acad. Sci.*, 1950, **31**, 450.
10. ——— and Ramachandran, G. N. *Ibid.*, 1951, **34**, 240.

LIGHT SCATTERING IN SOAP-SOLVENT SYSTEMS

Depolarisation Factors of Transversely Scattered Light in Sodium Oleate-Xylene Systems During and After Gel-Formation

By V. Sundaram

Received May 19, 1953
(Communicated by Dr. Mata Prasad, F.A.SC.)

Introduction

The utility of depolarisation measurements for investigating gel-forming systems is well known. Since the process of formation of soap gels in organic solvents has not been studied so far by such measurements, it was felt desirable to carry out a systematic study of the depolarisation of the transversely scattered light in sodium oleate and xylene systems during and after setting and also the effects of concentration, temperature and syneresis.

Experimental Details

A. Preparation of the gel-forming systems

Gel-forming solutions containing 0·5% and 1·5% sodium oleate in xylene were prepared by weighing out the requisite amount of the soap in a Pyrex test tube of internal diameter 1·5″, adding 75 c.c. of xylene and heating in an oil-bath as described elsewhere (Prasad and Sundaram, 1951). The test tube with the solution was heated to 130° C. and then transferred to the observation bath in which measurements were made.

B. Optical arrangements

Sunlight reflected by means of a heliostat mirror and condensed by a long focal length lens ($f = 45$ cm.) provided with an iris diaphragm placed in a dark room was used to make the depolarisation measurements. The beam of light was focussed at the centre of a test tube containing the gel-forming system and kept immersed in the centre of a beaker containing 'Nujol' which served as a bath. The depolarisation measurements were carried out by the well-known Cornu method using incident unpolarised light, and light with its vibrations vertical and horizontal respectively. Suitable apertures were provided for the incident and transmitted beams and the transversely scattered radiation, and adequate precautions were taken to cut off all stray light and minimise errors in measurement (Rao, 1927;

Prasad *et al.*, 1949, 1952). Since, even with the maximum aperture (5 cm.) the error due to the finite convergence (Ananthakrishnan, 1935) was extremely small, no corrections were made.

C. (i) *Measurements while cooling the soap-solvent systems*

The temperature of the Nujol in the bath (beaker) was initially maintained at 130° C., the same as the gel-forming solution. The measurements of the depolarisation factors were made using incident light unpolarised and polarised with vibrations vertical and horizontal. The bath and the system were then allowed to cool at an average rate of 1° C. for every two minutes. At suitable temperatures the temperature of the system was maintained constant and the depolarisation factors measured.

(ii) *Measurement of the effect of temperature on the depolarisation in soap-xylene systems*

For this purpose the temperature of the bath was kept constant at 70° C. and the test tube containing the gel-forming solution was transferred to this bath. The depolarisation measurements were made when the temperature of the system reached 70° C. Similarly measurements were made also at 50° C. and 30° C., each time using however a freshly prepared sample of gel-forming solution.

(iii) *Measurement of the effect of syneresis*

The measurements of the depolarisation factors of the gel set in the bath at 30° C. were carried out after 24 hours, 48 hours, and 96 hours to determine the effect of syneresis on the depolarisation values.

D. Measurement of gelation temperature of soap-solvent gel-forming systems

A test tube containing the gel-forming solution of sodium oleate in xylene free from bubbles was closed by a cork through which a thermometer was introduced. After heating it in the paraffin-bath to 130° C. it was transferred to a thermostat maintained at 30° $\pm$ ·1° C. By slightly tilting the system at various intervals, the exact temperature at which it set to gel, *i.e.*, the gelation temperature, was determined. Several measurements were made for the same system, every time using a fresh solution and in each successive measurement the number of times the gel was disturbed was reduced so that a correct value of the gelation temperature was obtained.

Results

The depolarisation factors observed during the cooling of sodium oleate-xylene systems were plotted against temperature and the values interpolated

TABLE I

Concentration of Sodium Oleate = 0·5%

Gelation temperature = 78° C.

Temperature °C.	ρ_h	ρ_v	ρ_u	$\rho_u = \frac{1+1/\rho_h}{1+1/\rho_v}$	$\Delta\rho_e = \rho_u - \frac{2\rho_v}{1+\rho_v}$
130	92·0	3·0	6·5	6·1	0·7
120	87·5	3·0	7·0	6·2	1·2
110	82·0	3·5	8·0	7·5	1·2
100	76·0	4·5	10·5	10·0	3·0
90	69·0	6·0	14·3	13·9	3·0
80	62·5	8·0	19·5	19·3	4·7
70	55·8	10·5	28·5	26·5	7·4
60	49·0	13·5	38·3	36·2	12·0
50	42·0	18·0	50·5	51·6	20·0
40	40·5	21·8	63·0	62·0	26·4

TABLE II

Concentration 1·5%

Gelation temperature = 90° C.

Temperature °C.	ρ_h	ρ_v	ρ_u	$\rho_u = \frac{1+1/\rho_h}{1+1/\rho_v}$	$\Delta\rho_e = \rho_u - \frac{2\rho_v}{1+\rho_v}$
130	93·0	3·0	6·5	6·0	0·7
120	87·8	3·0	6·5	6·2	0·7
110	82·3	3·5	7·8	7·5	1·0
100	77·0	4·5	10·3	9·9	1·7
90	71·5	6·8	14·5	15·3	1·9
80	66·0	9·3	20·3	21·3	2·3
70	60·3	12·8	29·0	30·2	6·3
60	55·0	18·5	43·0	44·0	11·8
50	50·8	25·3	61·0	59·9	20·7
40	47·3	27·8	67·8	67·7	24·3

TABLE III

Temperature °C.	ρ_h	ρ_v	ρ_u	$\Delta\rho_u = \rho_u - \frac{2\rho_v}{1+\rho_v}$
	(*a*) Concentration 0·5%			
70	54·8	10·6	27·1	8·0
50	42·2	18·9	52·8	21·0
30	39·0	22·8	65·6	28·6
	(*b*) Concentration 1·5%			
70	57·8	12·5	29·5	7·2
50	49·0	26·0	63·3	22·1
30	43·8	29·5	70·4	24·9

TABLE IV

Time hours	ρ_h	ρ_v	ρ_u	$\Delta\rho_u = \rho_u - \frac{2\rho_v}{1+\rho_v}$
	(*a*) Concentration 0·5%			
0	39·0	22·7	65·6	28·5
24	36·1	23·8	73·0	34·5
48	34·7	23·8	74·3	35·8
96	32·0	24·9	75·6	35·8
	(*b*) Concentration 1·5%			
0	43·8	29·5	70·4	24·8
24	42·2	30·7	75·6	28·6
48	40·6	31·4	78·3	30·5
96	39·0	32·0	81·1	31·5

from these curves at definite temperatures are given in Tables I and II. Table III gives the effect of temperature on depolarisation and in Table IV is listed the depolarisation factors during the syneresis of these gels. Fig. 1 represents the variation of $\Delta\rho_u$ with temperature for the concentration corresponding to Table I.

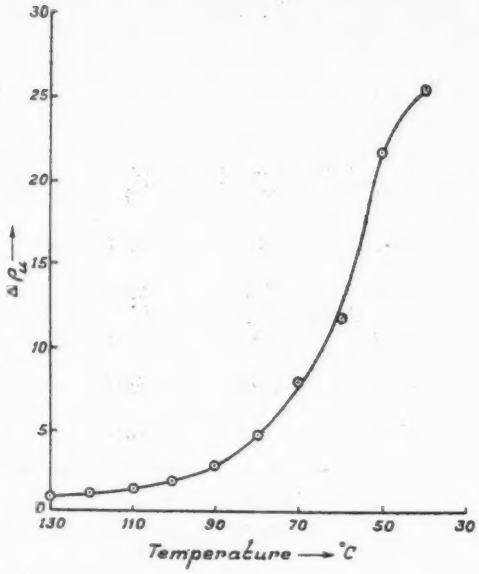

FIG. 1

DISCUSSION OF RESULTS

From Tables I and II it is seen that with decrease of temperature from 130° C., ρ_h which is originally high, continuously decreases, while ρ_v and ρ_u which are small in the beginning increase when the systems are cooled to their respective gelation temperatures and continue to do so even below these. A decrease in the value of ρ_h indicates an increase in the size of the particles and the magnitude of ρ_v is indicative of the anisotropy of the particles. Also it is known that an increase in the size of the particles in any scattering medium causes an increase in the value of $\Delta\rho_u$, which is the difference between the observed value ρ_u and the anisotropic part of ρ_u which can be considered equal to $2\rho_v/(1+\rho_v)$ (Sivarajan, 1951). Consequently it can be concluded that the particles in the system which are initially small and nearly spherical, increase both in size and anisotropy during and after gelation.

These observations may be explained on the basis of the existing theory of the formation of soap gels in organic solvents. It is well known that sodium oleate forms molecular solutions in organic solvents (Lawrence, 1938; Prasad *et al.*, 1945) at temperatures near about the boiling points of the solvents and this state is maintained for a short range of temperature

when the solutions are cooled. Consequently ρ_h is high and ρ_v is low. As the solutions are cooled further, the systems undergo saturation at first and then supersaturation causing the formation of colloidal particles which agglomerate at still lower temperatures. The aggregation of the particles is shown by the decrease in the values of ρ_h and increase of $\Delta\rho_u$. The formation of anisotropic particles at lower temperatures shown by the increasing value of ρ_v, is probably due to the fibrillar nature of the soap molecules as revealed by electron microscope photographs.

A soap-solvent system sets to a gel at its gelation temperature due to certain equilibrium conditions prevailing in the system at that temperature. In the gel a part of the dispersion medium which is a saturated solution of the soap in the solvent at that temperature, is attached to the soap particles due to solvation while the remaining is held within the interfibrillary spaces. When the set gel is cooled below its gelation temperature, the decrease in solubility of the soap in the solvent at lower temperatures throws out some more soap from the dispersion medium. These particles may aggregate themselves or get attached to the already existing particles and thereby cause the observed changes in the values of the depolarisation factors after setting.

The depolarisation measurements show that similar changes with time are observed in gels of different concentrations and the ρ_v values are slightly higher in gels of higher concentration indicating thereby that at the higher concentration the particles are more anisotropic. However the values of $\Delta\rho_u$ are not very much different for the two concentrations studied, revealing thus that the final size of particles is not appreciably altered by change in concentration.

It will be seen from Table III that the final values of ρ_h are smaller and those of ρ_u, ρ_v and $\Delta\rho_u$ are larger for gels set at lower temperatures than for the gels set at higher temperatures. These observations are in agreement with those noticed during the slow cooling from 130° C. and indicate that the particles of the gels set at higher temperatures are smaller and less anisotropic than those of the gels set at lower temperatures.

As stated earlier the particles in the system undergo large changes in size and anisotropy when the gels are allowed to cool from their gelation temperatures to 30° C. These arise from the fact that some more particles of soap are thrown out of the dispersion medium. These changes cause the instability of the structure formed at the gelation temperature and syneresis results on account of the displacement of the system to attain stability at the lower temperature (Prasad and Sundaram, 1951). On the

other hand, only slight changes in size and anisotropy take place when the gels are kept at 30° C. for some time and these indicate that the second stage of syneresis is a slow process compared to the first.

A comparison of the final values of ρ_v in the gels studied with those of gelatin and agar (Katti, 1948, 1949) show that the particles in gels of sodium oleate in xylene are more anisotropic. While the final values of ρ_u in the case of most inorganic gels is less than 40% (Ramaiah, 1937; Prasad *et al.*, 1944, 1949, 1952; Kanekar and Subramanian, 1952; Desai and Sundaram, 1953), in the gels under consideration they are over 60%. These observations show that the structure of the particles in the gel-forming systems of sodium oleate in xylene is very different from that of particles in inorganic gel-forming systems and in aqueous systems of gelatin and agar.

ACKNOWLEDGMENT

The author desires to express his sincere thanks to Dr. Mata Prasad, D.SC., F.N.I., F.R.I.C., F.A.SC., for his valuable advice and suggestions and to the authorities of the University of Bombay for the award of a Research Studentship which enabled him to carry out the present investigation.

SUMMARY

The depolarisation factors ρ_u, ρ_v and ρ_h of the light transversely scattered from sodium oleate-xylene systems have been measured during and after gel-formation. It has been observed that the particles in these systems increase in size and anisotropy during and after gel-formation. The observed results have been explained on the basis of the existing theory of the formation of soap gels in organic solvents. The size of particles in these gels does not seem to depend on the concentrations of the gel-forming systems.

REFERENCES

1. Ananthakrishnan, R. .. *Proc. Ind. Acad. Sci.*, 1935, **2A**, 133.
2. Desai, R. L. .. *J. Univ. Bombay*, 1953, **22**, pt. 3, 24.
3. ——— and Sundaram, V. *Ibid.*, 1953, **22**, pt. 3, 8.
4. Kanekar, C. R. and Subramanian, K. E. *Ibid.*, 1951, **19**, pt. 5, 28.
5. Katti, P. K. .. *Proc. Ind. Acad. Sci.*, 1948, **28A**, 216; 1949, **30A**, 35.
6. Lawrence, A. S. C. .. *Trans. Faraday Soc.*, 1938, **34**, 660.
7. Prasad, M. and Guruswamy, S. *Proc. Ind. Acad. Sci.*, 1944, **19A**, 47, 66, 77.

8. Prasad, M., Hattiangdi, G. S. and Vishvanath, C. V. *Ibid.*, 1945, **21A**, 90, 105.
9. ——— and Doss, K. D. V. *J. Colloid Sci.*, 1949, **4**, 349.
10. ——— and Sundaram, V. *Proc. Ind. Acad. Sci.*, 1951, **33A**, 305.
11. ———— .. *Ibid.*, 1951, **33A**, 333.
12. Prasad, M., Subramanian, K. E., Desai, R. L. and Kanekar, C. R. *J. Colloid Sci.*, 1952, **7**, 178.
13. Ramaiah, K. S. .. *Proc. Ind. Acad. Sci.*, 1937, **5A**, 138.
14. Rao, I. R. .. *Ind. J. Phys.*, 1927, **2**, 61.
15. Sivarajan, S. R. .. *Curr. Sci.*, 1951, **20**, 202.

A MAGNETO-OPTIC METHOD FOR THE DETERMINATION OF PIEZO-OPTIC COEFFICIENTS

By S. Ramaseshan

(*Department of Physics, Indian Institute of Science, Bangalore-3*)

Received September 29, 1954

(Communicated by Prof. R. S. Krishnan, F.A.SC.)

1. Introduction

When a cubic crystal or a glass is stressed, it becomes birefringent and the measurement of the relative retardation produced, gives some of the linear combinations of the piezo-optic constants q_{ij}. In particular, in glasses one gets the quantity $(q_{11}-q_{12})$. For the measurement of the relative retardation a Babinet Compensator is often used. While the measurements with a Babinet Compensator are very accurate the instrument is not too well suited for the measurement of the dispersion of the piezo-optic coefficients. From the recent studies on the magneto-optic rotation in birefringent media by the author (1949, 1951) a simple method has been developed for the measurement of the relative retardation produced on stressing an isotropic solid. The particular merit of the method is not so much its accuracy as its convenience for the measurement of the dispersion of the piezo-optic coefficient with wavelength.

This paper gives the experimental details and the theory of the method. Preliminary studies have been made of the piezo-optic coefficients of some glasses and they compare well with the determinations made with the Babinet Compensator (Vedam, 1950).

2. Theory of the Method

When plane polarised light is incident on a birefringent crystal (or a stressed isotropic solid) placed in a magnetic field, the emergent light is elliptically polarised. The major axis of the emergent ellipse is in general, inclined at an angle ψ to the plane of vibration of the incident light. This inclination is dependent on the angle which the incident electric vector makes with the principal planes of vibration of the crystal. In the particular case when the two are parallel, ψ is given by

$$\tan 2\psi = \frac{\sin 2\gamma \sin \Delta}{\cos^2 2\gamma + \sin^2 2\gamma \cos \Delta}, \qquad (1)$$

where $\Delta = \Delta_0 t = t\sqrt{\delta_0^2 + (2\rho_0)^2}$ and $\tan 2\gamma = \frac{2\rho_0}{\delta_0}$

Δ_0 is the composite phase retardation per unit length, $\delta = t\delta_0$ the total phase retardation when there is no magnetic field and $\rho = t\rho_0$ the total rotation when there is no birefringence and t the thickness of the specimen.

It has been shown (Ramaseshan, 1951) that by suitable algebraic manipulation, when δ_0 and $2\rho_0$ are small, equation (1) could be written as

$$2\psi = 2\rho \left\{1 - \frac{\delta^2}{3!} + \frac{\delta^2}{5!}\left[(m^2+6)(2\rho)^2\right] - \frac{\delta^2}{7!}\left[(m^4+120\,m^2-90)(2\rho)^4\right] - \cdots\right\} \tag{2}$$

here $m = \dfrac{1}{\sin 2\gamma} = \dfrac{\Delta}{2\rho} = \dfrac{\sqrt{\delta^2+(2\rho)^2}}{2\rho}$

In the case when δ and 2ρ are very small the equation (2) reduces to

$$2\psi = 2\rho\left(1 - \frac{\delta^2}{6}\right) \tag{3}$$

As both ρ and ψ can be accurately measured with the aid of a half shade, these formulæ could be used in determining the stress-optic coefficients in isotropic solids. One measures the magnetic rotation when the solid is not stressed and again the apparent rotation with the same magnetic field and a known applied stress. Then the birefringence introduced δ, can be evaluated from equation (2) or (3). When δ and 2ρ are both less than 20° equation (3) gives an accuracy of about 1% in the value of δ. On the other hand for higher values of δ and 2ρ equation (2) must be used. In calculating δ by equation (2) the method of successive approximation must be resorted to in evaluating the value of m. By taking the four terms of the series given in equation (2) one could get the value of δ within 1% of its true value (when $\delta < 55°$ and $2\rho < 40°$).

In the earlier experiments one peculiarity was met with. When the solid was stressed the values of ψ determined for the magnetic field on and reversed, differed considerably. This was found to be due to the fact that the incident electric vector did not exactly coincide with the direction of the stress in the solid. Experimentally also, setting them exactly parallel was extremely difficult, particularly as the direction of stress in the experimental solid was never exactly the same at all points. Detailed mathematical investigation of the problem of *the dependence of ψ on the inclination of the electric vector to the principal axes of strain* has shown (Ramachandran and Ramaseshan, 1952) that the usual practice of taking the mean of the measurements for the two directions of the magnetic field practically eliminates the errors caused by the slight mis-setting of the polariser or specimen or as a result of the variation of the stress axis in the specimen. In fact when

the setting was out by 3° (a case hardly to be met with in practice) while the individual readings for the two directions of the field varied by about 10% the mean value deviated from the correct value by less than 1%.

3. EXPERIMENTAL PROCEDURE AND RESULTS

The usual Faraday effect arrangement with a half shade at the polarizer end was used in the measurement of ρ and ψ. A simple lever arrangement made of brass was employed to stress the specimen (in the present case a glass block 3 cm. × 3 cm. × 2 cm.). The light traversed the 2 cm. side of the glass block. Pressure was transmitted to the specimen by lead blocks suitably shaped to make the stress direction in the central portion almost vertical and the stress distribution fairly uniform. Some care was taken in setting the electric vector of the incident polarised beam parallel to the stress direction. It was found best to measure ρ and ψ for two or three different field strengths but for the same value of stress and later to repeat the measurements for different stresses. Table I gives a typical set of values obtained for one of the glasses (glass No. 10). δ in each case was calculated from formula (2) using 3 terms. It may be mentioned here that while the 4th term practically does not affect the values of δ, the omission of the 3rd term introduces an error of the order of 6% in the last three determinations.

TABLE I

Stress in Kgwt./mm.^{2}	Field in Oersteds	2ρ in degrees	2ψ in degrees	δ in degrees
0·091	6420	13·26	13·03	19·0
0·091	9490	19·62	19·27	19·0
0·179	6420	13·28	12·30	38·0
0·179	9490	19·60	18·21	39·1
0·268	6420	13·30	11·32	56·0
0·268	9490	19·60	16·71	56·5

Table II gives the results of the measurements made on 12 optical glasses. $[\delta_0]$ represents the path retardation introduced by a pressure of 1 dyne/cm.^{2} for λ 5893 when the thickness of the substance is 1 cm. and the values of $(p - q)$ are calculated from the formula

$$\delta = \frac{n^2}{2R}(p - q)P$$

where δ represents the birefringence introduced, R the rigidity modulus, n the refractive index for λ 5893, P the stress in dynes per sq. cm. and p and q the Neumann's strain-optical constants. The values of R obtained by Vedam (1950) for the same set of glasses have also been entered in the table. The last two columns give the values of $(p - q)$ obtained in the present studies as well as those obtained by Vedam (1950) who used the classical Babinet Compensator method.

One notices from Table II that the values obtained by the magneto-optic method are quite in agreement with those obtained by the Babinet Compensator method. The method could therefore be confidently used for the study of the variation of $(p - q)$ with wavelength. In doing so, it must be borne in mind that 2ρ must never be greater than 40°.

TABLE II

Glass* No.	n_D	$R \times 10^{-11}$ in dynes/cm.^{2}	$[\delta_0] \times 10^{13}$	$(p - q)$ (Author)	$(p - q)$ (Vedam)
1	1·4669	1·878	4·24	0·074	0·0762
2	1·4934	2·538	4·13	0·094	0·0918
3	1·5023	2·862	3·07	0·078	0·0774
4	1·5093	2·917	4·18	0·107	0·1049
5	1·5171	3·354	3·09	0·090	0·0909
6	1·5300	2·275	4·50	0·087	0·0875
7	1·5269	2·604	3·54	0·079	0·0771
9	1·5700	3·053	3·55	0·088	0·0855
10	1·5699	2·474	3·52	0·069	0·0698
11	1.5895	3·292	2·42	0·061	0·0633
12	1·5981	2·404	3·51	0·066	0·0642
13	1·6062	2·569	3·06	0·061	0·0630

* The numbering of these Jena glasses is the same as that adopted by Dr. R. S. Krishnan (*Proc. Ind. Acad. Sci.*, 1936, 4, 211).

It is found most convenient to make the measurements from λ 7000 to λ 4500 visually and to use a spectrographic or a photomultiplier technique for lower wavelengths. Such techniques have been developed in this laboratory (V. Sivaramakrishnan) and the result of measurements for different wavelengths on glasses and other isotropic solids will be reported later. It is

found that although the error in the absolute value of $(p - q)$ may be as great as 3 to 4% the relative values for different wavelengths would be of very much greater accuracy.

The author's thanks are due to Dr. K. Vedam for the discussions he had with him and also to Prof. R. S. Krishnan for his kind interest in the work.

4. SUMMARY

A simple magneto-optic method for the measurement of the relative retardation produced on stressing an isotropic solid is described. The method is based on the determination of the true and apparent magneto-optic rotation of the isotropic solid in the unstressed and the stressed states. The method is found to be useful in the measurement of the dispersion of the piezo-optic coefficients with wavelentgh.

REFERENCES

1. Ramaseshan, S. .. *Doctorate Thesis, Nagpur University*, 1949.
2. ———— .. *Proc. Ind. Acad. Sci.*, 1951, **34**, 32, 97.
3. ——— and Chandrasekharan .. *Curr. Sci.*, 1951, **20**, 150.
4. Ramachandran, G. N. and Ramaseshan, S. *J.O.S.A.*, 1952, **42**, 49.
5. Vedam, K. .. *Proc. Ind. Acad. Sci.*, 1950, **31**, 450.

1430–54 Printed at The Bangalore Press, Bangalore City, by C. Vasudeva Rao, Superintendent, and Published by The Indian Academy of Sciences, Bangalore.

NOTICE TO AUTHORS

Scientific papers intended for publication in the *Proceedings of the Indian Academy of Sciences* can be accepted only when they are communicated by a Fellow of the Academy whose duty shall be to satisfy himself that such communications are fit to be read at the Meeting of the Academy and published in its *Proceedings*.

Papers should not ordinarily exceed fifty pages of foolscap. MSS. should be either typewritten or written in legible hand on one side of the paper. All papers should be carefully revised by the authors and should be absolutely in final form for printing. Position for text-figures should be indicated. Each paper shall conclude with a critical summary not exceeding 350 words.

Drawings, diagrams or other illustrations should be made on larger scale (preferably) twice the size than the ones in which they are intended to appear. They should be done in Indian ink on bristol board with lettering in pencil. Scale of magnification of camera lucida tracings should be indicated by the side of drawings. In certain special cases arrangements will also be made for monochrome lithographic and other colour plates. Reduction of illustrations desired should be indicated in pencil. Appropriate legends should accompany all drawings. Names of authors are to be marked in pencil on the left-hand corner of drawing sheets. Photomicrographs should be securely mounted with colourless paste.

All tables, quotations and footnotes which will be set hereafter (beginning from Vol. I, No. 2) in types smaller than the text, should be typewritten on separate sheets and placed with the text in proper sequence. Footnotes should be numbered in Arabic numerals.

References to literature in the text should be given, whenever possible, in chronological order, only the names of authors and years of publication, in brackets, being given. They should be cited in full after the summary, the authors' names following in alphabetical order. Thus,

Name or Names of author; Name of Journal (abbreviation) with a single underline; Year of publication; Number of Volume with a double underline, and lastly page. The following would be a useful illustration:—

Bergmann and Stather . . . . . Z. Physiol. Chem., 1926, 152, 189.

Two copies of slip-proof and wherever possible, a page proof for final revision will be sent to authors. All corrections are best made on the slip-proof which should be transmitted to the Office of the Academy. All proof corrections involve heavy expenses which would be negligible if the papers are carefully revised by the authors before submission.

Authors will be supplied with reprints of their papers at cost price, if intimation is given at the time of returning the slip-proof.

Blocks appearing in the *Proceedings* will be available for purchase by their respective authors. Orders for the same should be sent along with the corrected proofs and in any case not later than one month after the date of publication of the paper. The price charged would be 25% of the actual cost of the blocks *plus* freight and despatching charges. If the blocks are reproduced in other journals or publications, due acknowledgment should be made in them to the *Proceedings*.

The original drawings and plates of blocks appearing in the *Proceedings* will be returned to such of the authors as may require them provided the cost of despatching such originals is borne by them.

CONTENTS

PAGE

On the Construction of Large Nuclear Emulsion Block Detectors . . . . . R. R. Daniel, G. Friedmann, D. Lal, Yash Pal and B. Peters 151

Intermediate Layers of Ionisation between the E and F_1 Layers of the Ionosphere over Ahmedabad (23°N, 72°·6 E) . . . . . R. G. Rastogi 158

Photoelastic Studies of Optically Active Crystals. $NaClO_3$ and $NaBrO_3$ . . . . . T. S. Narasimhamurty 167

Light Scattering in Soap-solvent Systems—Depolarisation Factors of Transversely Scattered Light in Sodium Oleate-Xylene Systems During and After Gel-Formation . . . . . V. Sundaram 176

A Magneto-optic Method for the Determination of Piezo-optic Coefficients . . . . . S. Ramaseshan 184